

# Trends of carbon fluxes and climate over a mixed temperate–boreal transition forest in southern Ontario, Canada



Norma Froelich<sup>a</sup>, Holly Croft<sup>b</sup>, Jing M. Chen<sup>b</sup>, Alemu Gonsamo<sup>b</sup>, Ralf M. Staebler<sup>c,\*</sup>

<sup>a</sup> Earth, Environmental and Geographical Sciences Department, Northern Michigan University, Marquette, MI 49855, USA

<sup>b</sup> Department of Geography and Program in Planning, University of Toronto, Toronto, ON M5S 3G3, Canada

<sup>c</sup> Air Quality Processes Research Section, Environment Canada, Toronto, ON M3H 5T4, Canada

## ARTICLE INFO

### Article history:

Received 23 January 2015

Received in revised form 27 May 2015

Accepted 31 May 2015

Available online 17 June 2015

### Keywords:

Net ecosystem productivity

Gross ecosystem productivity

Ecosystem respiration

Eddy covariance

Mixed forest

Long-term change

## ABSTRACT

The exchanges of carbon dioxide (CO<sub>2</sub>), water vapor, and energy were measured nearly continuously since 1996 over a mixed mature transition forest at the Borden Forest Research Station, in southern Ontario, Canada. Borden Forest, one of the longest running flux towers in North America, is located in the temperate–boreal ecotone. This transitional region, which includes species close to the limits of their environmental range, may be particularly susceptible to changes in forest composition as a result of climate change. Here we analyze net CO<sub>2</sub> exchange, measured using the eddy covariance method, and concurrent meteorological variables. The forest was found to be a low-to-moderate CO<sub>2</sub> sink, with uptake of  $177 \pm 28 \text{ gC m}^{-2} \text{ yr}^{-1}$  (mean  $\pm$  standard error). In two of the years, however, the forest was a weak CO<sub>2</sub> source (i.e., 1996:  $-36 \text{ gC m}^{-2} \text{ yr}^{-1}$  and 2001:  $-35 \text{ gC m}^{-2} \text{ yr}^{-1}$ ), demonstrating that the forest can switch between source and sink. Over the 17 years of measurement, annual net ecosystem productivity (NEP) increased by  $15.7 \text{ gC m}^{-2} \text{ yr}^{-1} \text{ yr}^{-1}$ , due to a decline in ecosystem respiration of  $4.2 \text{ gC m}^{-2} \text{ yr}^{-1} \text{ yr}^{-1}$  and an increase in gross ecosystem productivity of  $11.6 \text{ gC m}^{-2} \text{ yr}^{-1} \text{ yr}^{-1}$ . There were notable long-term indications of climatic warming: annual air temperature rose by  $0.09^\circ \text{C yr}^{-1}$ , while soil temperature increased by  $0.08^\circ \text{C yr}^{-1}$ . Photosynthetically active radiation and soil temperature were found to be the dominant environmental drivers of interannual variations and long-term trends in NEP; on seasonal or monthly time-scales, air temperature and precipitation also influenced CO<sub>2</sub> uptake. NEP is positively correlated with the length of the net carbon uptake period, which varied from 111 to 164 days. The large interannual variations in CO<sub>2</sub> flux in this dataset demonstrate the need for long time series of CO<sub>2</sub>, water vapor, and energy fluxes, together with meteorological measurements; such measurements show long-term trends, which can be used to understand and predict future changes in forest-atmosphere exchanges in response to anticipated changes in climate.

Crown Copyright © 2015 Published by Elsevier B.V. All rights reserved.

## 1. Introduction

Forests play a crucial role in the global carbon (C) cycle through the sequestration of large amounts of C from the atmosphere (Beer et al., 2010). Pan et al. (2011) estimated that global forest stocks of  $861 \pm 66 \text{ PgC}$  (42% in live biomass, 44% in the upper 1 m of soil, 8% in deadwood, and 5% in litter) are increasing at  $2.4 \pm 0.4 \text{ PgC yr}^{-1}$ . Yet, there is a need for better accounting of regional budgets and projections of how climate change may affect C stocks and their fluxes. This requires thorough quantification and description of net ecosystem productivity (NEP) and its component parts –

gross ecosystem productivity (GEP) and ecosystem respiration ( $R_E$ ) – and the biophysical and climatic influences on them. Much work has been done on these problems in recent decades. Eddy covariance measurements indicate that NEP in forests ranges from 750 to  $-150 \text{ gC m}^{-2} \text{ yr}^{-1}$  (Yi et al., 2010), with mature forests generally close to being CO<sub>2</sub> neutral (Coursolle et al., 2012). However, forests can quickly change from an annual C sink to a C source, as uptake is affected by such factors as species composition, age structure, environmental conditions, and exposure to disturbance (Baldocchi, 2008; Luysaert et al., 2008). The interannual variability of NEP has been attributed to a number of variables, including: spring rainfall (Allard et al., 2008), land surface phenology (Richardson et al., 2009), seasonal air temperature (Barr et al., 2007; Hollinger et al., 2004), summer drought (Granier et al., 2007), forest disturbance (Baldocchi, 2008), snow conditions (Nobrega and Grogan, 2007), and carbon uptake phenology, particularly in autumn (Wu

\* Corresponding author at: Air Quality Processes Research Section, Environment Canada, 4905 Dufferin Street, Toronto, ON M3H 5T4, Canada.

E-mail address: [ralf.staebler@ec.gc.ca](mailto:ralf.staebler@ec.gc.ca) (R.M. Staebler).

et al., 2013). While considerable progress has been made, uncertainties still remain regarding the spatial distribution of C sinks, the interannual variability of NEP, the complex interrelationships of GEP and  $R_E$  with environmental and ecosystem controls, and, ultimately, the vulnerability of C pools (Baldocchi, 2008; Luysaert et al., 2008; Pan et al., 2011). There continues to be a need for additional measurements to better assess the interannual variability in fluxes and to understand the ecophysiological processes, as well as the climatic and biophysical controls on these processes. Long-term eddy covariance measurements are particularly well-suited for this purpose (Baldocchi, 2008; Barr et al., 2007; Zha et al., 2013).

The Borden Forest Research Station offers many possibilities for such research. Borden Forest is in the Great Lakes–St. Lawrence forest ecotone, which extends across eastern North America between 44 and 47°N. This forest ecotone is a transition zone containing both southern temperate forest species (e.g., red maple (*Acer rubrum*), red oak (*Quercus rubra*), eastern white pine (*Pinus strobus*)) and northern boreal species (e.g., black spruce (*Picea mariana*) and jack pine (*Pinus banksiana*)), many of which are at or near the limits of their temperature and moisture ranges (Goldblum and Rigg, 2005, 2010; Leithead et al., 2010). Consequently, this transitional region is identified as being particularly susceptible to climate change, and may experience substantial changes in forest composition, with northward migration of temperate species into boreal forest, as a result of small variations in climate (Fisichelli et al., 2013; Frelich and Reich, 2010; Leithead et al., 2010). Long-term datasets of carbon budgets and their drivers are required to better understand which environmental and climatic factors affect forest composition and what impacts these changes in species composition will have on carbon budgets, especially in light of a changing global climate.

Borden Forest Research Station has been the site of eddy covariance measurements of carbon dioxide, water, and energy fluxes for almost two decades. This makes the Borden site an important contributor among the group of long-term flux tower sites located in predominantly deciduous forests; other such sites include Harvard Forest, USA (Goulden et al., 1996), Takayama Forest, Japan (Saigusa et al., 2002), the Southern Old Aspen site, Canada (Black et al., 2000) and the Walker Branch forest, USA (Greco and Baldocchi, 1996). Previous investigations of forest–atmosphere exchange at Borden Forest have been reported for the periods 1995–1998 (Lee et al., 1999) and 1996–2003 (Teklemariam et al., 2009). This paper extends the analysis from 1996 to 2013. The availability of such an extensive near-continuous dataset makes it possible to examine longer term trends and to draw more robust conclusions about the main environmental controls on forest productivity. The aims of this paper are: (1) to investigate the changing patterns of both  $CO_2$  exchange and meteorological variables across monthly, seasonal, annual, and multi-year time scales and (2) to identify the environmental and climatic drivers of interannual  $CO_2$  flux variability at this mixed temperate forest.

## 2. Materials and methods

### 2.1. Borden Forest Research Station

The Borden Forest Research Station, hereafter referred to as Borden Forest, is located in a mixed deciduous and coniferous boreal–temperate transition forest near the southern tip of Georgian Bay in southern Ontario (44°19'N, 79°56'W) in the Great Lakes/St. Lawrence forest region (Fig. 1). According to tree surveys conducted in 1995 (Lee et al., 1999) and 2006 (Teklemariam et al., 2009), red maple (*A. rubrum*) accounts for approximately 50% of the stems in the forest; Eastern white pine (*P. strobus*), large-tooth and trembling aspens (*Populus grandidentata* and *Populus tremuloides*), white and red ash (*Fraxinus americana* and *Fraxinus pennsylvanica*),



Fig. 1. Location of the Borden Forest flux tower site, within the deciduous-boreal ecotone. Source: Goldblum and Rigg (2010).

and American beech (*Fagus grandifolia*) are among the other main species. The forest is a natural regrowth from farmland abandoned in the early 20th century. Mean canopy height is 22 m and the leaf area index has been measured to be between 4.1 and 5.1  $m^2 m^{-2}$  in mid growing season (Neumann et al., 1989; Staebler et al., 2000; Teklemariam et al., 2009). Over the last 15 years, mean annual temperature at the site was 7.4 °C and mean annual total precipitation was 784 mm.

The flux tower is located near the northern edge of a tract of forest approximately 5 km wide, surrounded by agricultural lands. The fetch of largely uninterrupted forest extends to distances of 1.5–4 km in southeastern and southwestern quadrants, and to 1000 m in the northeastern direction; however, in the northwest quadrant, there are extensive grass- and crop-lands at distances as small as ~400 m. The topography within a 4 km radius of the tower is relatively flat. On length-scales on the order of a few hundred meters, the terrain slopes by 1–2 m (downslope toward the northeast). On shorter length-scales, however, larger variations in elevation do occur, including a river valley of 20 m depth and 40 m width, approximately 1 km south of the tower and a small stream valley of 5 m depth and a few 10s of m width, approximately 100 m south of the tower.

### 2.2. Instrumentation

The main measurement platform is a tower instrumented for eddy covariance and profile measurements (44 m tall from 1995 to 2003; the replacement tower constructed at the same location in 2004 is 42 m tall). Details on instrumentation can be found in Appendix A.

Measurements of turbulent fluctuations of wind velocity, temperature, water vapor, and  $CO_2$  – used in computing ecosystem fluxes – are made at a height of 33 m using a sonic anemometer (Kaijo Denki prior to 2001, CSAT from 2001 to 2003, and ATI K-type since 2004) coupled with a closed-path infrared gas analyzer (IRGA, LI-COR Li-6262). The IRGA is located in a temperature-controlled hut at the base of the tower; air is drawn from an inlet ~0.5 m from the anemometer to the IRGA at a rate of 20 L/min, sufficient to maintain turbulent flow. Both the IRGA and the anemometer are operated at 10 Hz.

Meteorological measurements that have been made since 1995 include: temperature and relative humidity at two heights (33 and 41 m); temperature at 12 heights (from 1.5 to 44 m); incoming photosynthetically active radiation (PAR) and shortwave radiation (both at 44 m until 2003, then at 41 m); net global radiation (at 33 m); wind speed and direction (at 44 m); and barometric pressure (at 2 m). Additional meteorological instruments were added more recently, including: 4-component incoming & outgoing radiation (33 m), downwelling PAR transmitted through the canopy to a height of 1.5 m, and reflected PAR (see Appendix A for dates

of instrument installations or changes). A gas profile system was installed in 2001 to measure concentrations of water vapor, CO<sub>2</sub>, O<sub>3</sub>, and SO<sub>2</sub> at six heights (1.5–41 m); using a manifold system, air from the six intakes is sequentially sampled and diverted to three instruments (LI-COR Li-6262 IRGA, Thermo 49 O<sub>3</sub> analyzer, and Thermo 43 SO<sub>2</sub> analyzer). Soil temperature profiles (from 5 to 100 cm depth) are measured at two locations with a combination of thermocouples and thermistors; soil heat flux plates are installed at a depth of 7 cm at each of these profile sites. Soil moisture profiles are measured at two locations (depths from 2 to 100 cm). Finally, bole temperatures are measured in two trees (red maple and aspen) at heights of 2, 5, and 9 m.

### 2.3. Flux calculations

Eddy covariance fluxes are determined as the covariance between the vertical velocity component and the fluctuating scalar of interest. The fluxes, as well as means and standard deviations of all velocity components and scalars, are computed for every half-hour. Computation of the Borden Forest gas fluxes was performed by a data processing program developed at SUNY Albany. Spikes that fall outside  $\pm 10$  standard deviations from the mean within each half-hour were identified and eliminated. Mean values of the six de-spiked time series (three components of velocity, sonic temperature, and CO<sub>2</sub> and H<sub>2</sub>O mole fractions) were computed and subtracted from the half-hour time series to calculate perturbation values ( $w'$ ,  $C'$  etc.). The standard deviation of each variable and all covariances were determined from these time series of de-spiked perturbation values.

The sensible heat flux ( $Q_H$  [W m<sup>-2</sup>]) was calculated from the vertical turbulent flux of the temperature ( $\overline{w'T'}$  [K m s<sup>-1</sup>]) as:

$$Q_H = \rho_{\text{air}} \overline{w'T'} \quad (1)$$

where  $\rho_{\text{air}}$  is the density of air and  $c_p$  is the specific heat capacity of air. The density of air is computed from the air temperature at 33 m and the atmospheric pressure. The air temperature perturbations ( $T'$ ) were determined from the sonic temperature, with corrections for moisture fluctuations (all years) and momentum fluctuations (Kaijo-Denki anemometer, only), following Schotanus et al. (1983)

Gas fluxes were corrected for density effects due to water vapor fluctuations following Webb et al. (1980), (hereafter WPL). WPL corrections for temperature fluctuations were not needed, as these were effectively removed by the heated sample line and closed-path analyzer located in a temperature-controlled hut. The latent heat flux ( $Q_E$  [W m<sup>-2</sup>]) was calculated from the WPL-corrected vertical turbulent flux of water vapor mole fraction ( $\overline{w'H_2O'_{WPL}}$ ) as:

$$Q_E = \frac{\rho_{\text{air}} L_v \overline{w'H_2O'_{WPL}} M_{H_2O}}{M_{\text{air}}} \quad (2)$$

where  $L_v$  is the latent heat of vaporization of water and  $M_{H_2O}$  and  $M_{\text{air}}$  are the molar masses of water and air, respectively. The CO<sub>2</sub> flux ( $F_{CO_2}$  [ $\mu\text{mol m}^{-2} \text{s}^{-1}$ ]) was calculated from the WPL-corrected vertical turbulent flux of the CO<sub>2</sub> mole fraction ( $\overline{w'CO_{2WPL}'}$ ) as:

$$F_{CO_2} = \frac{\rho_{\text{air}} \overline{w'CO_{2WPL}'}}{M_{\text{air}}} \quad (3)$$

The net ecosystem exchange (NEE [ $\mu\text{mol m}^{-2} \text{s}^{-1}$ ]) was calculated as the sum of  $F_{CO_2}$ , the vertical CO<sub>2</sub> flux at 33 m, and  $S_{CO_2}$ , the change of CO<sub>2</sub> storage. Horizontal turbulent fluxes and both vertical and horizontal advection of CO<sub>2</sub> were assumed to be negligible (Staebler and Fitzjarrald, 2004). The storage change in the layer below 33 m was estimated as the vertical integral of the rate of

change of CO<sub>2</sub> concentration with time ( $t$ ):  $S_{CO_2} = \int_0^{33\text{m}} \frac{\Delta CO_2}{\Delta t} dz$ . This

estimate was made using the gas profile measurements when available or using the single-point measurement of CO<sub>2</sub> from the eddy covariance sensor at 33 m, when profile data were unavailable.

### 2.4. Data quality assessment and analysis

All data (means, standard deviations, and covariances from the flux system and means of meteorological, gas profile, and soils data) were inspected for sensor drift, instrument malfunction, calibration problems, or outliers. Calibrations or drift corrections were applied when possible; outliers and data involving instrument malfunction were removed from the dataset. In addition, some data were removed from the dataset at times when field notes indicated work was done on or near an instrument. Computed fluxes were rejected if the mean or standard deviation of either base variable of that flux (velocity, temperature, H<sub>2</sub>O, or CO<sub>2</sub>) was rejected from the dataset. Major causes of data loss included instrument or computer failures or bad weather. While the fetch of uninterrupted forest at Borden is generally >2000 m to the south of the tower, to the northwest there are some extensive areas of agricultural fields or grasslands, as close as 400 m to the tower. With the short fetch, the fluxes measured on the tower may not be representative of the forest processes; therefore, all data observed when wind direction was >285° or <20° were filtered out.

Eddy covariance measurements are well known to systematically underestimate nighttime ecosystem fluxes during stable, low wind conditions when turbulence is poorly developed. A common approach to this problem is to filter data using a friction velocity threshold ( $u_{*Th}$ ), below which measured NEE is assumed unrepresentative of ecosystem activity. To objectively determine an appropriate threshold for Borden Forest, we use the change point detection method of Barr et al. (2013). Annual  $u_{*Th}$  values ranged from 0.24 to 0.40 m s<sup>-1</sup> with typical 95% confidence intervals of  $\sim 0.15$  m s<sup>-1</sup>. These annual estimates were pooled across years, to give a value of  $0.3 \pm 0.15$  m s<sup>-1</sup>. This threshold value is higher than previously reported for this site (Lee et al., 1999; Teklemariam et al., 2009). There was some seasonal variation in the threshold with values as low as 0.2 m s<sup>-1</sup> in summer and averaging 0.4 m s<sup>-1</sup> in winter. However, as the winter season has the smallest NEE values, errors introduced by using too low of a  $u_{*Th}$  threshold on winter NEE data are expected to be small; thus, no attempts were made to use seasonally-dependent thresholds to filter the data.

### 2.5. Energy balance closure

A common check of the quality of the flux data is the energy balance closure – the balance between net radiation minus storage heat flux and the turbulent energy fluxes measured using the eddy covariance system. The storage heat flux calculated for Borden Forest includes: soil heat flux, bole heat flux, change in sensible and latent heat storage in the air volume below the EC system, and energy consumption during photosynthesis (following Blanken et al. (1997) for photosynthetic energy consumption and Oliphant et al. (2004) for all other fluxes). Including all terms, the energy balance closure at Borden Forest was between 66% and 90%, in each of the 17 years, averaging 75%. These values are not atypical of Fluxnet sites (e.g., Blanken et al. (1997) observed closure of 87% for 1 year, while Oliphant et al. (2004) observed 72% closure over 4 years). Interannual variability of the energy closure was primarily due to the uncertainty in latent heat flux. The energy balance closure at Borden was slightly higher in summer months than in

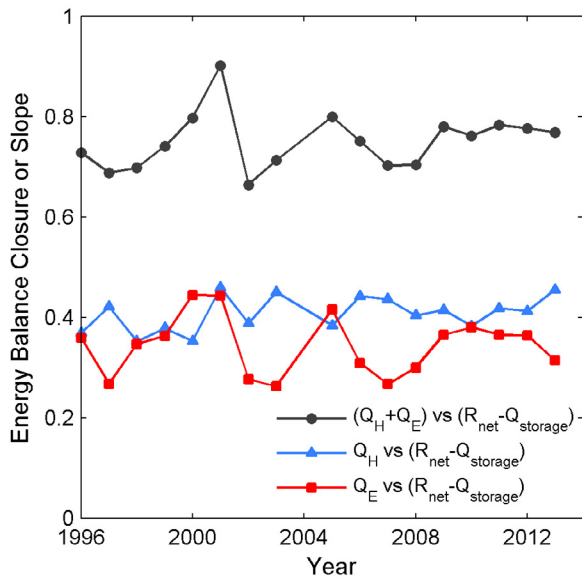


**Fig. 2.** Annual variations in the energy balance closure, determined as the slope, using all available half-hourly values, of the sum of the sensible ( $Q_H$ ) and latent ( $Q_E$ ) turbulent heat fluxes and the available energy, ( $R_{net} - Q_{storage}$ ). The partitioning of available energy is indicated by the slope of each of  $Q_H$  and  $Q_E$  vs ( $R_{net} - Q_{storage}$ ).  $Q_{storage}$  includes ground heat flux, bole heat storage, latent and sensible heat storage in the air volume below the EC system, and photosynthetic energy consumption.

winter months; however, there was no significant trend from year to year (Fig. 2).

On a seasonal basis, variability in the heat storage was largely due to both the ground heat flux and the photosynthetic energy consumption, while heat storage in the boles or air volume below 33 m had minimal contributions (Fig. 3a). On a diel basis, all terms contributed to the heat storage (Fig. 3b and c). Oliphant et al. (2004) made similar observations at Morgan–Monroe State Forest regarding the contributions of soil, bole, and air heat fluxes to energy storage. Inclusion of all five terms, rather than just the soil heat storage improved the energy balance closure by 5–8% (relative to available  $R_{net} - Q_{storage}$ ) in all years. This supports the inclusion, when possible, of all terms, not only the ground heat flux.

### 3. Analysis

#### 3.1. Gap-filling

Gaps in meteorological data were filled using statistical relations of the Borden Forest data to data from a weather station at Egbert, located 15 km to the southeast of the Borden site. The meteorological variations at the two sites were found to be quite similar. A linear regression of half-hourly temperatures at the two sites yielded a slope = 0.98 and  $R^2 = 0.99$ , while linear regressions of half-hourly daytime solar radiation had  $R^2 = 0.93$  with a slope =  $2.0 \mu\text{mol m}^{-2} \text{s}^{-1} / (\text{W m}^{-2})$  when comparing PAR to shortwave radiation and a slope = 1.0 when comparing shortwave radiation to shortwave radiation.

Gaps in the  $\text{CO}_2$  flux data were filled using the model described in Barr et al. (2004). Using this method, net ecosystem productivity ( $\text{NEP} = -\text{NEE}$ ) was partitioned between gross ecosystem productivity (GEP) and ecosystem respiration ( $R_E$ ).  $R_E$  was estimated as  $-\text{NEP}$ , when GEP is zero during nights and/or cold seasons (defined as having both air and 5 cm soil temperatures below  $0^\circ\text{C}$ ). Respiration

was empirically modeled as the product of a logistic function of soil temperature, and a time-dependent coefficient,  $r_w(t)$ :

$$R_E = r_w(t) \hat{R}_{E0}(T_s) = \frac{r_w(t) r_1}{(1 + \exp\{r_2(r_3 - T_s)\})} \quad (4)$$

The coefficient  $r_w(t)$  was determined, within a 100-half-hour-point moving window, as the slope of a linear regression, forced through the origin, of the model  $\hat{R}_{E0}$  and the measured respiration. Gaps in nighttime and cold-season  $R_E$  were filled and all warm-season daytime  $R_E$  values were estimated using Eq. (4).

GEP was estimated during warm-season daytime periods as  $\text{NEP} + R_E$ . From these estimates, GEP was empirically modeled as the product of a Michaelis–Menten type light response curve,  $\hat{\text{GEP}}_0(\text{PPFD})$ , and a time-dependent coefficient,  $p_w(t)$ :

$$\hat{\text{GEP}} = p_w(t) \hat{\text{GEP}}_0(\text{PPFD}) = \frac{p_w(t) A_{\text{max}} \text{PPFD}}{\text{PPFD} + k} \quad (5)$$

The coefficient  $p_w(t)$  was determined, within a 100-point moving window, as the slope of a linear regression forced through zero, of the modeled  $\hat{\text{GEP}}_0$  and measured gross productivity. Gaps in daytime warm-season GEP were filled using Eq. (5), while nighttime and/or cold-season GEP was assumed to be zero. All gaps in NEP were filled as  $\text{GEP} - R_E$ .

Both time-dependent functions,  $r_w$  and  $p_w$ , were determined within moving windows of fixed number (100) of available half-hour points, rather than fixed length in time, with the computed slope assigned to the mean time of the 100 points; between these assigned times,  $r_w$  and  $p_w$  were estimated via linear interpolation.

## 4. Results

#### 4.1. Monthly and annual variations in environmental variables

Monthly and annual climatic variations over the 17 year measurement period are shown in Fig. 4 (note: there are no data for 2004 due to instrument and tower replacement). The average annual air temperature during these 17 years was  $7.4^\circ\text{C}$ ,  $\sim 0.9^\circ\text{C}$  warmer than the 30-year (1981–2010) normal at the nearby Cookstown, Ontario climate station. Annual air temperatures increased by  $0.09^\circ\text{C yr}^{-1}$  ( $R = 0.52$ ;  $p < 0.05$ ); summer (June–August) air temperatures increased by  $0.10^\circ\text{C yr}^{-1}$  ( $R = 0.51$ ,  $p < 0.05$ ), while winter (November–March) temperatures increased by  $0.08^\circ\text{C yr}^{-1}$  ( $R = 0.25$ ,  $p > 0.05$ ). Monthly mean winter air temperatures throughout the 17 years displayed greater range than summer temperatures. Precipitation averaged 784.6 mm annually, with 314.4 mm in the June–September growing season. While there was considerable variability both between years and between months, there were no significant trends in either annual or growing season precipitation. The driest year was 2007, with a total annual precipitation of 631 mm and only 146.6 mm during the growing season, less than half the summer average over all years. The wettest year (2008) had a total annual precipitation of 1006 mm, more than 85 mm higher than any other year; both 2000 and 2008 had particularly wet summers, with nearly 50% more precipitation than the summer average. Vapor pressure deficit (VPD) displayed strong intra-annual variations, with maximum values occurring in summer months, but no overall trends at decadal time-scales. Photosynthetically active radiation (PAR) varied greatly from month to month, with the winter of 1996/1997 having very low average PAR ( $49 \mu\text{mol m}^{-2} \text{s}^{-1}$ ) and the summers of 2007 and 2012 having higher than normal averages. Summer maximum values increased slightly, leading to the mean annual PAR increasing by  $2.47 \mu\text{mol m}^{-2} \text{s}^{-1}$  per year ( $R = 0.69$ ,  $p < 0.001$ ) over the 17 year time period. Annual mean soil temperatures increased at  $0.08^\circ\text{C yr}^{-1}$  ( $R = 0.71$ ,  $p < 0.001$ ). Although soil moisture had a large

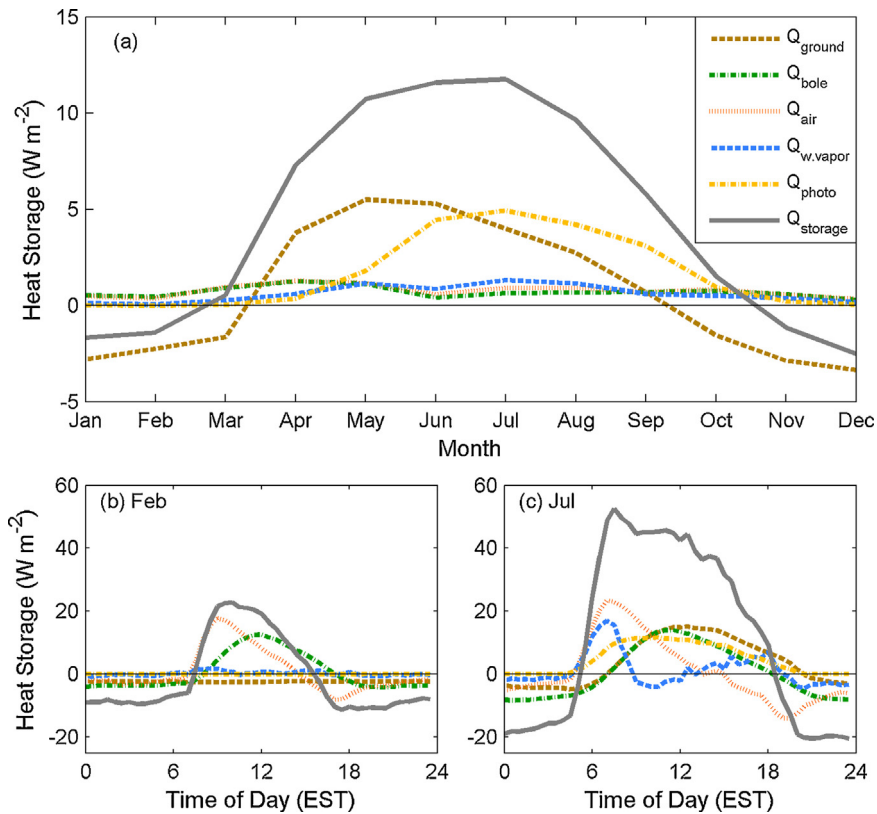


**Fig. 3.** Monthly means (a) and diel patterns for the months of February (b) and July (c) of the heat storage budget. Total heat storage ( $Q_{\text{storage}}$ ) is the sum of ground heat flux ( $Q_{\text{ground}}$ ), bole heat storage ( $Q_{\text{bole}}$ ), change of sensible ( $Q_{\text{air}}$ ) and latent ( $Q_{\text{w.vapor}}$ ) heat content in the air volume below the 33 m eddy covariance system, and photosynthetic energy consumption ( $Q_{\text{photo}}$ ). The monthly totals are dominated by  $Q_{\text{ground}}$  in winter and by  $Q_{\text{ground}}$  and  $Q_{\text{photo}}$  in summer. On an hourly basis, all terms contribute to the heat storage. Figures include all years 1996–2013.

amount of missing data during three years (1996, 1999, 2003), summertime values in the middle of the time period (2001–2007) were low, indicating summer droughts, followed by a very wet summer and fall in 2008. While the data indicate soil moisture may have increased slightly over the years ( $0.001 \text{ m}^3 \text{ m}^{-3} \text{ yr}^{-1}$ ,  $R=0.50$ ,  $p<0.05$ ), we cannot rule out that this trend may be instrumental drift; certainly, with temperatures increasing and precipitation remaining fairly constant, a decrease in soil moisture is expected, not an increase.

#### 4.2. Monthly, seasonal, and annual variations in CO<sub>2</sub> fluxes

Fig. 5 shows the monthly and annual totals of GEP,  $R_E$  and NEP for 1996–2013. Borden Forest was a net CO<sub>2</sub> sink over this time period (mean annual total NEP:  $177 \text{ gC m}^{-2} \text{ yr}^{-1}$ ), but was a weak source in two years (1996:  $-36 \text{ gC m}^{-2} \text{ yr}^{-1}$  and 2001:  $-35 \text{ gC m}^{-2} \text{ yr}^{-1}$ ). Over the 17 years, NEP had an increasing trend of  $15.7 \text{ gC m}^{-2} \text{ yr}^{-1} \text{ yr}^{-1}$  ( $R=0.75$ ,  $p<0.001$ ), with the largest annual NEP occurring in 2013 at  $372 \text{ gC m}^{-2} \text{ yr}^{-1}$ . Annual  $R_E$  showed a declining trend of  $4.2 \text{ gC m}^{-2} \text{ yr}^{-1} \text{ yr}^{-1}$  ( $R=-0.12$ ,  $p>0.05$ ), with a mean annual total  $R_E$  of  $1196 \text{ gC m}^{-2} \text{ yr}^{-1}$ . Annual GEP increased by  $11.5 \text{ gC m}^{-2} \text{ yr}^{-1} \text{ yr}^{-1}$  ( $R=0.39$ ,  $p>0.05$ ), with a mean annual value of  $1373 \text{ gC m}^{-2} \text{ yr}^{-1}$ . In 2007 and 2008, both GEP and  $R_E$  were considerably lower than other years; 2007 had an unusually dry growing season while 2008 was unusually wet throughout the year.

The monthly  $R_E$  totals varied considerably among the years, particularly in the growing season; July  $R_E$  during 2007 was  $98 \text{ gC m}^{-2} \text{ month}^{-1}$ , compared to July 2000, at  $304 \text{ gC m}^{-2} \text{ month}^{-1}$ . In contrast, the monthly GEP totals during the summer were relatively consistent throughout the 17 years, with

slight reductions in 2001–2008. In the spring and fall transition months (April–May and September–November), the interannual variability in monthly GEP was large relative to the monthly mean over the 17 years, indicating the variability in growing season dynamics. In winter months, both  $R_E$  and GEP showed less variation. Monthly summer NEP totals also varied between years, typically with an indirect relationship to  $R_E$  values. Extreme low values of NEP occurred in April or October/November of some years, as a result of respiration that started before or ended after GEP.

Seasonal totals for NEP,  $R_E$ , and GEP showed variability between years and notable trends over the 17-year time series (Fig. 6). The increasing trend in annual NEP is primarily due to summertime (JJA) increases of  $4.65 \text{ gC m}^{-2} \text{ month}^{-1} \text{ yr}^{-1}$  ( $R=0.81$ ,  $p<0.001$ ); winter (JFM) NEP decreased slightly through time ( $-0.65 \text{ gC m}^{-2} \text{ month}^{-1} \text{ yr}^{-1}$ ;  $R=-0.62$ ,  $p<0.005$ ). Summer (JJA) GEP increased over the time period ( $3.82 \text{ gC m}^{-2} \text{ month}^{-1} \text{ yr}^{-1}$ ;  $R=0.60$ ,  $p<0.005$ ), while summer (JJA) respiration, in contrast, showed considerable scatter and had no significant trend. For both GEP and  $R_E$ , lower values occurred during 2007 and 2008, which were unusually dry and wet, respectively (Fig. 4). In winter, the decreasing trend in NEP is associated with an increasing trend in  $R_E$  of  $0.49 \text{ gC m}^{-2} \text{ month}^{-1} \text{ yr}^{-1}$  ( $R=0.45$ ,  $p<0.05$ ), likely associated with observed increases in soil temperature.

Temporal ‘fingerprints’ show the variability in net ecosystem productivity (Fig. 7) over each day, over each year, and among years. Each fingerprint shows positive NEP values during growing season daylight hours, negative NEP (i.e., respiration) during growing season nighttime hours, and near-zero values of NEP during the winter and transition seasons. Yet, variability is evident in the magnitude of NEP within each growing season and among years. In recent

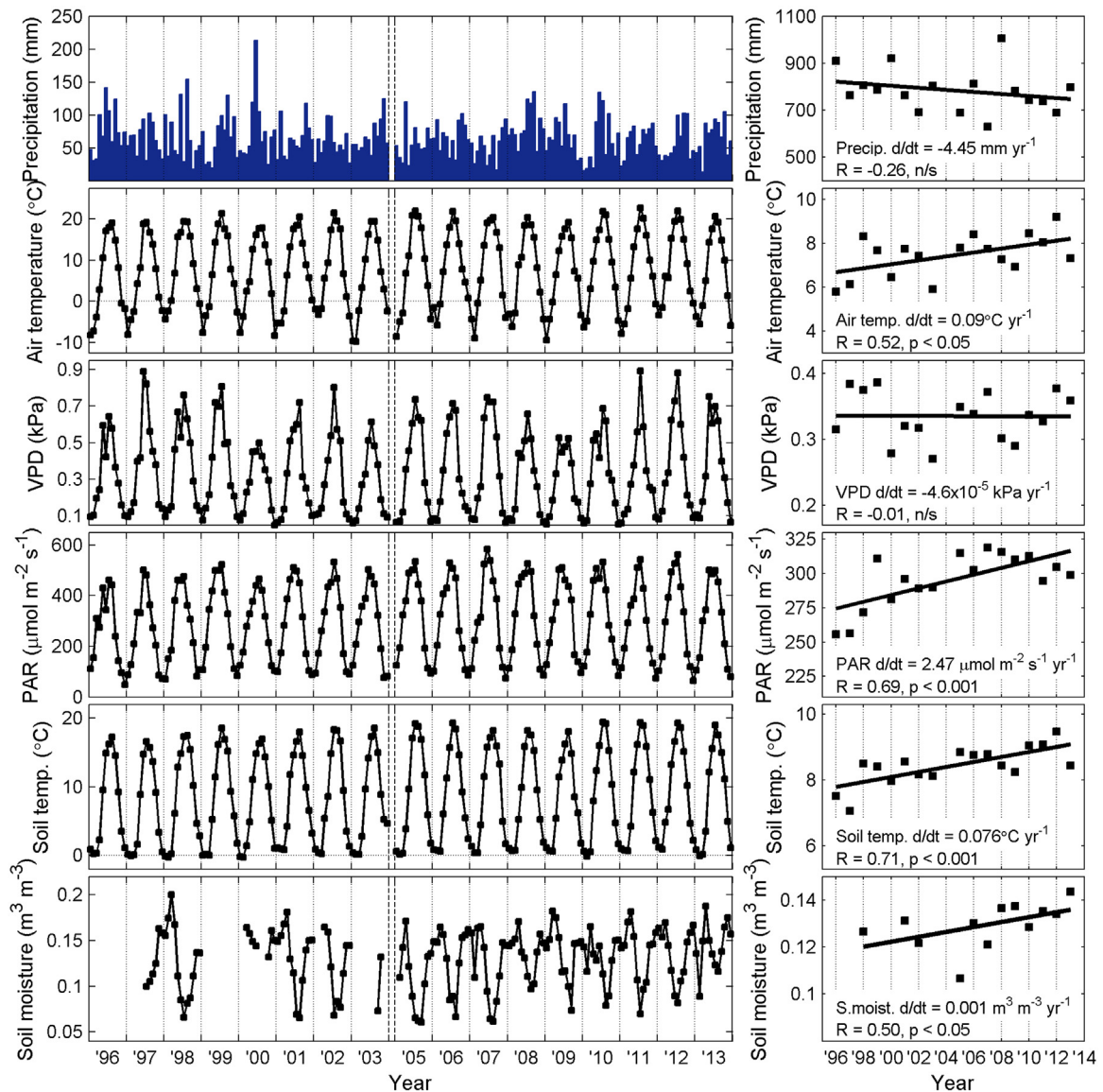


**Fig. 4.** Monthly (left) and annual (right) climate variables for the Borden Forest site, from 1996 to 2013. Precipitation data are monthly/annual totals, while all other variable show monthly/annual averages (including daytime and nighttime data for all variables). Note data for 2004 are absent. *n/s* = not significant.

years (especially 2009–2013), there has been an increase in the higher NEP values ( $>1.6 \text{ gC m}^{-2} \text{ h}^{-1}$ ), although larger values also occurred in 1997; however, there was no increase in low nighttime values ( $<-0.7 \text{ gC m}^{-2} \text{ h}^{-1}$ ). Interestingly, the two years with negative NEP values show very different temporal patterns, with 1996 having a short growing season with some higher NEP values and 2001 having a very long growing season with no high NEP values, due to high rates respiration. The blue band across the top of the positive NEP portion of some fingerprints (notably 2001) indicates a greater-than-normal lag of springtime GEP increase behind respiration increase. This is due to both warm early springtime temperatures driving increased respiration and/or a period of unusually low temperatures following bud-break that impede  $\text{CO}_2$  assimilation. Another notable observation is the very low summer night-time respiration contributions in 2007, indicated by the absence of a blue ring surrounding the positive NEP values (Fig. 6), coinciding with very low summertime precipitation and soil moisture levels (Fig. 4). These fingerprints emphasize the complexity of the forest response to the varying environmental conditions both within and among years.

#### 4.3. Carbon uptake period and annual carbon fluxes

Recent research has found relationships between interannual variations in carbon uptake metrics (e.g., growing season length or carbon uptake period), climate variability, and  $\text{CO}_2$  fluxes (Wang et al., 2011, 2012). Increases in the length of the growing season, either through an earlier spring or extended fall season, may result in increased primary productivity (Richardson et al., 2010). Three key seasonal carbon uptake period (CUP) metrics were derived from smoothed curves of daily NEP observations: the spring start (SCUP) and autumn end (ECUP) of the carbon uptake period were defined by the zero-crossings of the smoothed NEP time series from source to sink and sink to source, and the duration of carbon uptake period (DCUP) was calculated as the difference between those dates (Gonsamo et al., 2012, 2015; Wu et al., 2012).

The timing of the carbon uptake period varied considerably on an annual basis (dates listed in Fig. 7), with SCUP ranging from day of year (DOY) 124 to 159, ECUP varying from DOY 258 to 292, and the duration, DCUP, ranging from 111 to 164 days. Using only 1996–2012 data, Gonsamo et al. (2015) found that of these CUP

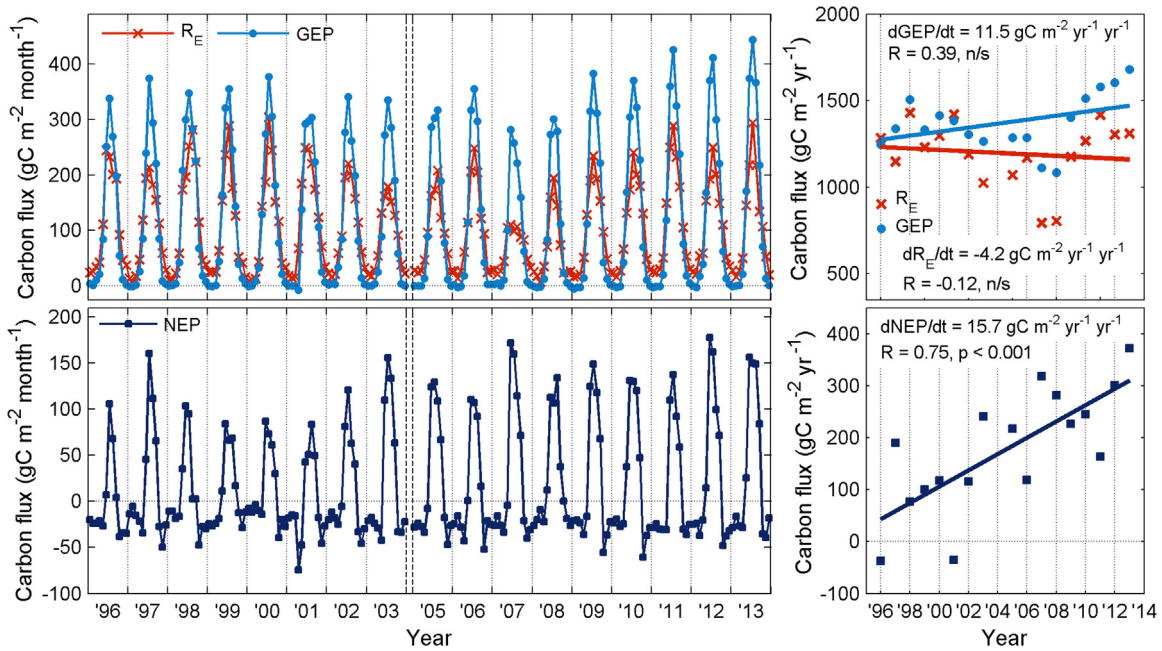


**Fig. 5.** Monthly (left) and annual (right) totals of gross ecosystem productivity (GEP), ecosystem respiration ( $R_E$ ), and net ecosystem productivity (NEP). Fluxes were estimated using data from wind directions  $20\text{--}285^\circ$  and  $u_* > 0.30 \text{ m s}^{-1}$ . Note data for 2004 are absent. *n/s* = not significant.

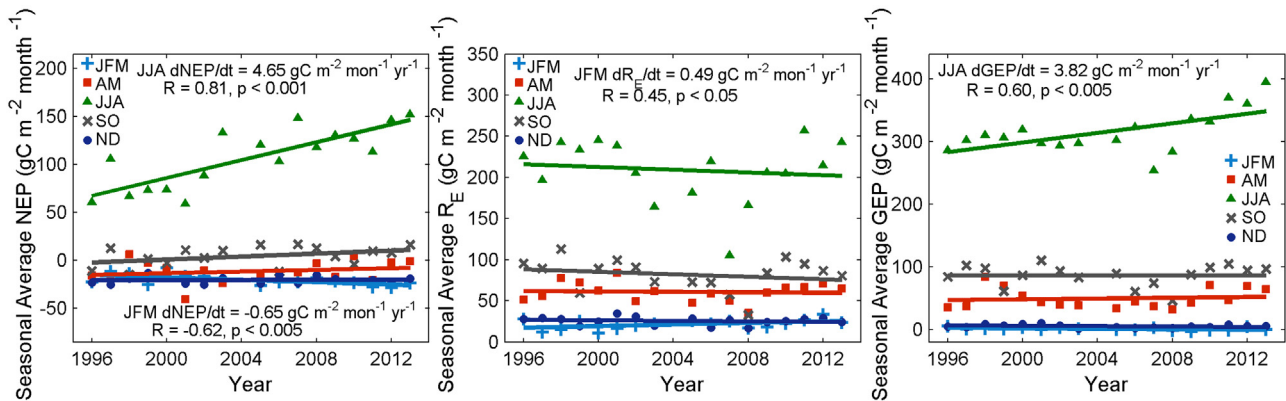


**Fig. 6.** Seasonal averages of net ecosystem productivity (NEP), ecosystem respiration ( $R_E$ ), and gross ecosystem productivity (GEP). For clarity, only significant trends are noted. Seasons are indicated by monthly abbreviations.

metrics, only the DCUP had a statistically significant ( $p < 0.05$ ) relationship with NEP. Here we extend the analysis, to include 2013 data and to compare the CUP metrics with GEP and  $R_E$  (Fig. 8). NEP increased with longer duration of the carbon uptake period (DCUP:  $R = 0.57$ ,  $p < 0.01$ ) and decreased with later start of the carbon uptake period (SCUP:  $R = -0.42$ ,  $p < 0.05$ ). Over the 17-year time series,  $R_E$  was significantly correlated with both the timing of the ECUP ( $R = -0.58$ ,  $p < 0.01$ ) and the duration of CUP ( $R = -0.44$ ,  $p < 0.05$ ). However, these correlations appear to be heavily influenced by very low respiration and late ECUP in the unusually dry year 2007 and the unusually wet year of 2008; if these years are removed from analysis,  $R_E$  is not significantly correlated with any of the CUP metrics. Using all available years, GEP showed no statistically significant relationship with any of the CUP metrics (Fig. 8); however, with the unusual years of 2007 and 2008 removed from the dataset, GEP was negatively correlated with SCUP ( $R = -0.48$ ;  $p < 0.05$ ), as might be expected.

Despite the large variation in carbon uptake timings (Fig. 8), the start, end, and duration of the carbon uptake period appear to have limited conclusive influence on the annual variability in

NEP and component fluxes. While the unusually dry and unusually wet years (2007 and 2008) are obvious counterpoints to any relationship between CUP metrics and carbon dioxide fluxes, we also note the large variability in growing season NEP across all years, as seen in the temporal ‘fingerprints’ (Fig. 7). Together, the poor correlations with CUP metrics and the variability in flux fingerprints demonstrate that it is inappropriate to use only simple indicators such as start/end dates of the growing season to explain year to year variations in annual carbon budgets. Other important factors include the intensity of the NEP values in the middle of the growing season, the decreased respiration rates during the drought years, and the early season temperatures after bud-burst.

#### 4.4. Intra-annual dependency of carbon exchange on environmental drivers

The Borden Forest long-term record allows analysis of variations in the temporal dependency of carbon exchange on environmental controls. Intra-annual patterns may be seen by comparing monthly NEP totals and monthly mean values of several environmental vari-

ables (Fig. 9). Correlation coefficient and significance are reported for the central growing season (JJA), the dormant winter season (ND, JFM), and the spring (AM) and fall (SO) transitional seasons between monthly CO<sub>2</sub> source and CO<sub>2</sub> sink.

Air and soil temperatures both showed a strong control on monthly NEP variations, with NEP generally remaining below zero in months with mean air temperature below 13 °C. Below this temperature, NEP averaged approximately  $-30 \text{ gC m}^{-2} \text{ month}^{-1}$ ,

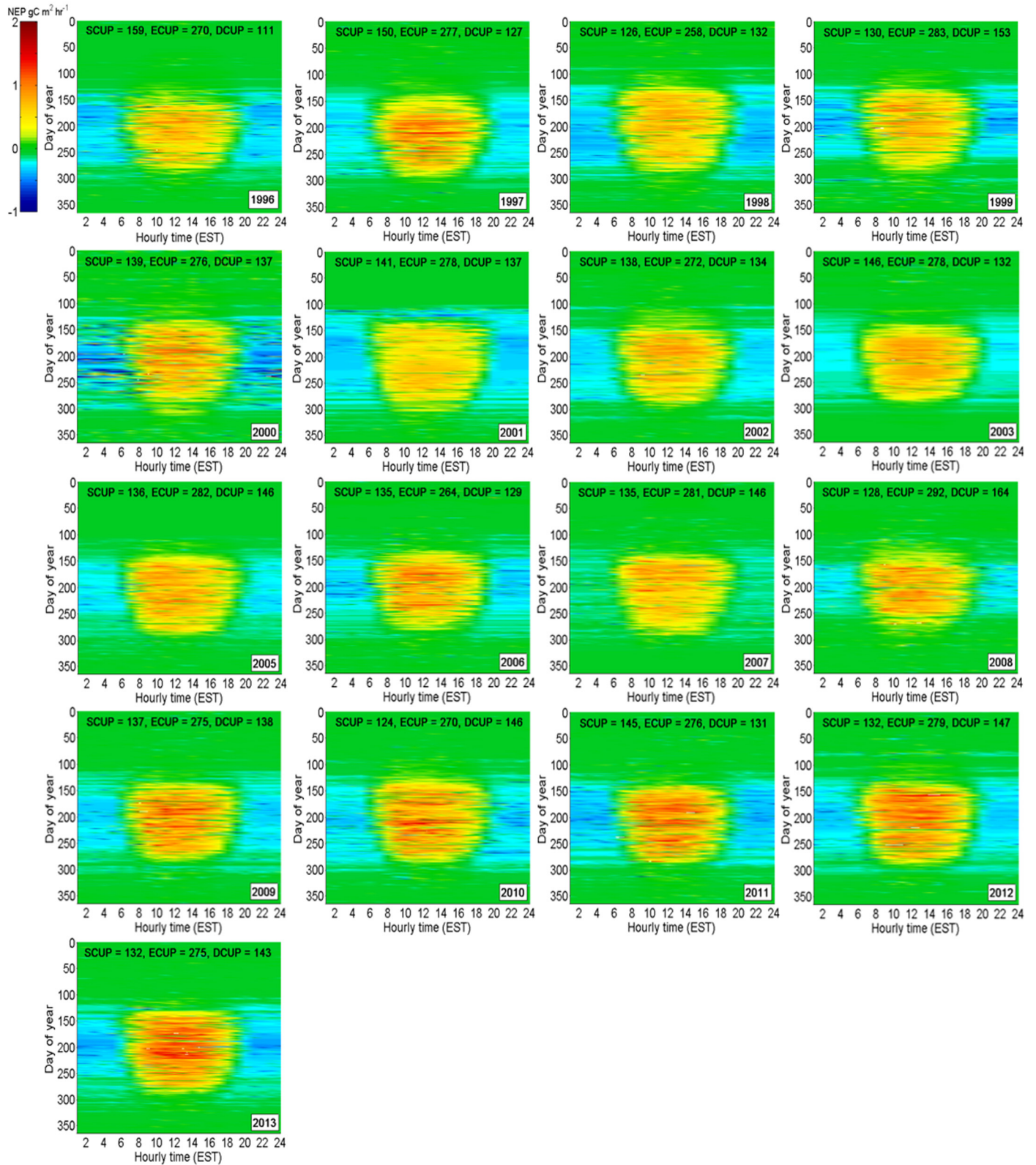


**Fig. 7.** Temporal ‘fingerprints’ show the net ecosystem productivity (NEP) for each hour of the day (x-axis) and each day of year (y-axis). Start (SCUP) and end (ECUP) dates and the duration (DCUP) of the carbon uptake period for each year are listed on each panel. (For interpretation of the references to color in the text, the reader is referred to the web version of this article.)



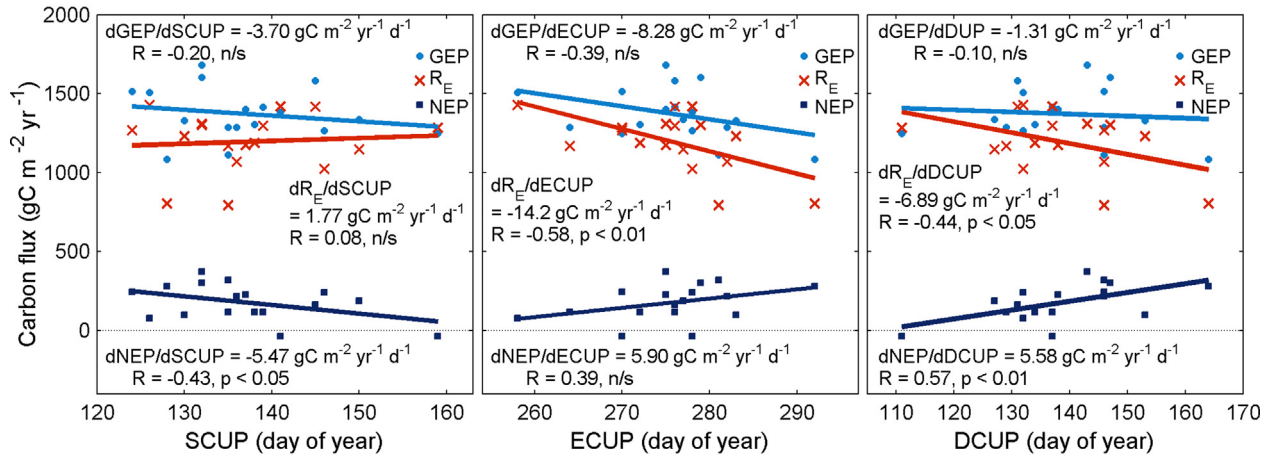


**Fig. 8.** Relationships of start of carbon uptake period (SCUP), end of carbon uptake period (ECUP), and duration of carbon uptake period (DCUP) to gross ecosystem productivity (GEP), ecosystem respiration ( $R_E$ ), and net ecosystem productivity (NEP). *n/s* = not significant.

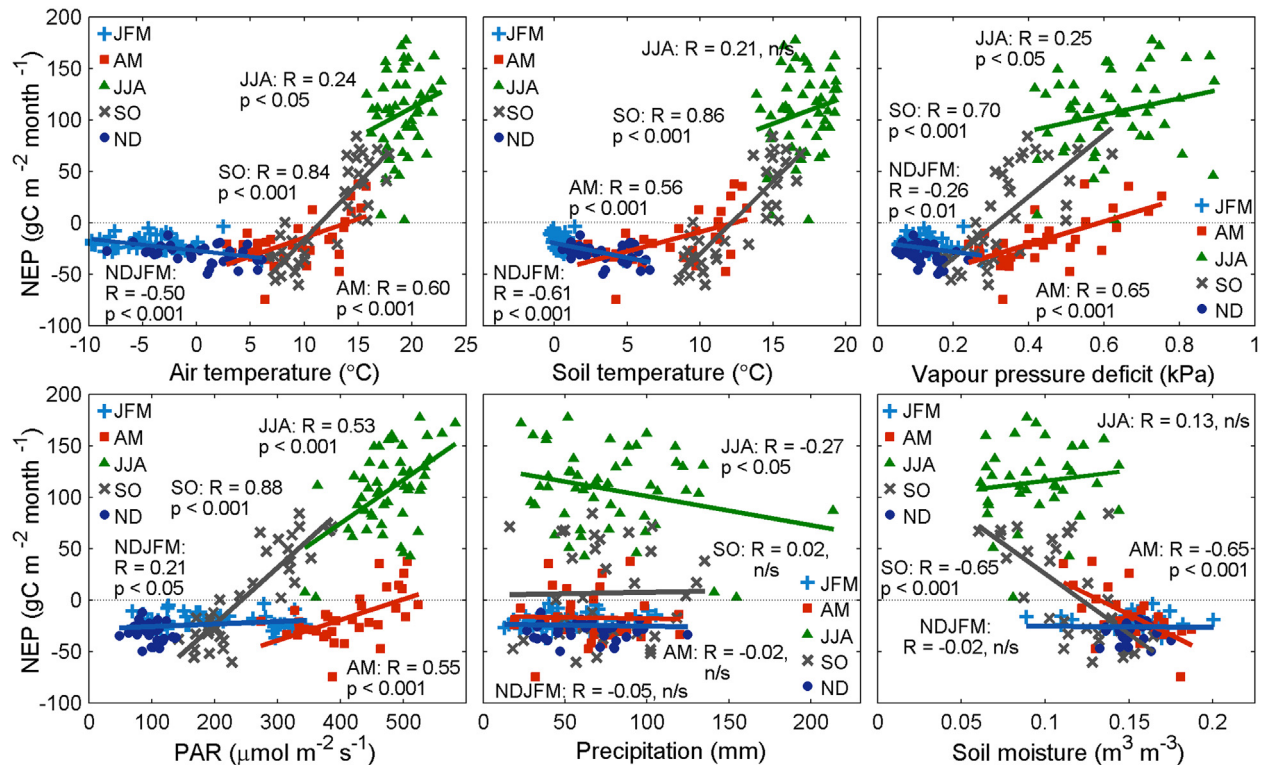


**Fig. 9.** Intra-annual relationships between net ecosystem productivity (NEP) and six environmental variables (air temperature, soil temperature, vapor pressure deficit, PAR, precipitation, and soil moisture). Each data point represents the total (NEP, precipitation) or average (all other variables) value for a month. Relationships are grouped by season, indicated by monthly abbreviations. *n/s* = not significant.

due to the dominance of  $R_E$  and limited contribution of GEP. In spring and fall, until 13 °C is reached, any change in temperature failed to result in a change in NEP. The relationships of NEP to VPD and PAR display an interesting temporal component with different responses in fall as compared to spring; this indicates an underlying hysteresis, affected by plant physiological factors or a dependence on other environmental controls (Niu et al., 2011). In the case of PAR, for example, the same light intensity did not lead to the equivalent NEP response in spring as it did in summer or fall months, which could be due to a delay in the photosynthetic efficiency in the spring, as chlorophyll is accumulating (Croft et al., 2014).

Fig. 9 also reveals that the dependence of NEP on different environmental factors varies among the seasons. NEP was most

strongly correlated with VPD ( $R = 0.65$ ,  $p < 0.001$ ) and air temperature ( $R = 0.60$ ,  $p < 0.001$ ) in spring months, with PAR ( $R = 0.53$ ,  $p < 0.001$ ) in summer months, and with PAR ( $R = 0.88$ ,  $p < 0.001$ ), soil temperature ( $R = 0.86$ ,  $p < 0.001$ ), and air temperature ( $R = 0.84$ ,  $p < 0.001$ ) in fall months. While precipitation showed a significant relationship with NEP only in summer ( $R = -0.27$ ;  $p < 0.05$ ), soil moisture appeared to be a secondary regulating factor in spring ( $R = -0.65$ ,  $p < 0.001$ ) and autumn months ( $R = -0.65$ ,  $p < 0.001$ ). In the winter months (ND/JFM), NEP decreased with increasing air temperature ( $R = -0.50$ ,  $p < 0.001$ ) and soil temperature ( $R = -0.61$ ,  $p < 0.001$ ), due to the temperature dependence of  $R_E$ . Wintertime NEP was also correlated with PAR ( $R = 0.21$ ;  $p < 0.05$ ) and VPD ( $R = -0.26$ ;  $p < 0.01$ ); however, these may reflect the complex rela-

**Table 1**

Interannual relationships (correlation coefficient  $R$ ) between seasonal net carbon fluxes (NEP,  $R_E$ , and GEP) and environmental variables, determined using seasonal totals (precipitation) or means (all other variables). Months are abbreviated by their first letter. Soil temperature is at 10 cm depth and soil moisture at 2–5 cm depth.

		Air temp (°C)	Soil temp (°C)	PAR ( $\mu\text{mol}/\text{m}^2/\text{s}$ )	VPD (kPa)	Precipitation (mm)	Soil moisture ( $\text{m}^3/\text{m}^3$ ) <sup>a</sup>	
NEP	JFM	0.01	-0.43*	-0.57**	0.02	0.49*	0.46	
	AM	0.50*	0.49*	0.41*	0.63**	-0.20	-0.44	
	JJA	0.40	0.45*	0.61**	0.21	-0.31	0.42	
	SO	0.39	0.39	0.53*	0.28	-0.04	-0.07	
	ND	0.03	0.31	0.30	0.01	0.32	0.23	
	Annual	0.19	0.35	0.53*	0.15	-0.24	0.20	
	JFM	0.07	0.50*	0.43*	0.17	-0.59**	-0.31	
	AM	0.42*	0.51*	0.13	0.37	-0.43*	-0.20	
	$R_E$	JJA	-0.18	-0.04	-0.48*	-0.14	0.34	0.21
		SO	-0.16	-0.14	-0.35	-0.08	-0.15	0.01
ND		0.08	-0.19	-0.11	0.16	-0.39	-0.26	
Annual		0.22	0.08	-0.42*	0.11	-0.04	0.27	
JFM		0.21	0.21	-0.31	0.50*	-0.29	0.19	
AM		0.68**	0.74**	0.40	0.74**	-0.47*	-0.50*	
GEP	JJA	0.16	0.37	0.02	0.03	0.09	0.54*	
	SO	0.05	0.08	-0.07	0.08	-0.20	-0.04	
	ND	0.20	0.10	0.23	0.31	-0.27	-0.15	
	Annual	0.39	0.33	-0.10	0.23	-0.22	0.44	

\*Significant at 95% confidence interval; \*\* significant at 99% confidence interval.

<sup>a</sup> Soil moisture results are from a reduced dataset (years with missing data: 1996, 1997, 1999 and 2003).

tionships of each variable with air or soil temperature or snow cover, rather than direct forcings. While these winter relationships are notable in terms of the strength of their correlation coefficients, it should be noted that the contribution of winter NEP to total annual  $\text{CO}_2$  flux is limited.

#### 4.5. Environmental controls on annual and seasonal carbon fluxes

The comparisons of monthly mean NEP with monthly means of environmental variables (Fig. 9) show the response of the ecosystem to changes across the seasons. However, the relationships depicted in Fig. 9 are dominated by differences between the months rather than by interannual differences (e.g., the difference between May and April temperatures in a given year tends to be as large, if not larger than, either the range of May temperatures or the range of April temperatures among years). To examine the influence of environmental drivers on the interannual variations in NEP,  $R_E$ , and GEP, we report correlation coefficients for seasonal mean environmental variables and  $\text{CO}_2$  fluxes, and also between annual mean values (Table 1). Total annual NEP has the strongest correlation with mean annual PAR ( $R=0.53$ ,  $p<0.05$ ). Annual  $R_E$  also had a significant relationship with PAR ( $R=-0.42$ ,  $p<0.05$ ), while annual GEP did not have any significant correlation with any of the environmental variables tested.

Correlations at seasonal time-scales also show notable differences. GEP is well-correlated with all environmental variables except PAR in spring (AM), but only correlated with soil moisture during summer (JJA) and did not correlate with any environmental variables in the fall (SO) transition period. Seasonal  $R_E$  results indicate the importance of air temperature, precipitation and soil temperature early in the year (JFM and AM) and of PAR in the growing season (JJA:  $R=-0.48$ ,  $p<0.05$ ). Strong negative correlations of precipitation with winter and spring  $R_E$  (JFM:  $R=-0.59$ ,  $p<0.01$ ; AM:  $R=-0.43$ ,  $p<0.05$ ) and spring GEP (AM:  $R=-0.47$ ,  $p<0.05$ ) may indicate the retarding influence of wintertime snow and spring rain on ecosystem processes. However, while these relationships are notable in the strength of their correlation coefficients, the contribution of winter and spring  $R_E$  and GEP to total annual  $\text{CO}_2$  uptake is limited. Seasonal NEP shows a shift from a dependence on air temperature ( $R=0.50$ ,  $p<0.05$ ), soil temperature ( $R=0.49$ ,  $p<0.05$ ) and VPD ( $R=0.63$ ,  $p<0.01$ ) early in the year (AM), to a dependence on PAR ( $R=0.61$ ,  $p<0.01$ ) and soil temperature ( $R=0.44$ ,  $p<0.05$ )

in summer (JJA) and a dependence only on PAR ( $R=0.53$ ,  $p<0.05$ ) in the fall (SO).

Summer seasonal mean GEP values displayed little correlation with summertime PAR or temperature over the 17 years (Table 1), whereas summer monthly mean values of these environmental variables were moderately correlated with summertime monthly GEP (air T:  $R=0.35$ ,  $p<0.01$ ; soil T:  $R=0.34$ ,  $p<0.01$ ; PAR:  $R=0.24$ ,  $p<0.05$ ; not shown), demonstrating the difference between using monthly (or shorter) time intervals binned by season (which show intra-annual patterns, Fig. 9) and seasonal time intervals (which better describe the interannual variability, Table 1).

## 5. Discussion

### 5.1. Long-term trends in annual NEP and ecosystem dynamics

The long time series at Borden Forest reveals an increasing trend in NEP (by  $15.7 \text{ gC m}^{-2} \text{ yr}^{-1} \text{ yr}^{-1}$ ), associated with a slightly increasing annual GEP ( $11.5 \text{ gC m}^{-2} \text{ yr}^{-1} \text{ yr}^{-1}$ ) and declining annual  $R_E$  ( $-4.2 \text{ gC m}^{-2} \text{ yr}^{-1} \text{ yr}^{-1}$ ). Over the 17-year time frame, Borden Forest was a moderate sink with net sequestration of  $177 \text{ gC m}^{-2} \text{ yr}^{-1}$ , comparable to other mature northern temperate forests. Studies of  $\text{CO}_2$  exchange over the temperate deciduous Harvard forest from 1992 to 2004 (Urbanski et al., 2007) showed a remarkably similar systematic increase in carbon sequestration amounting to  $15 \text{ gC m}^{-2} \text{ yr}^{-1} \text{ yr}^{-1}$ , which was attributed to changes in species composition and LAI. In the managed beech-dominated Sorø forest in Denmark, annual carbon sequestration was observed to increase by an average of  $23 \text{ gC m}^{-2} \text{ yr}^{-1} \text{ yr}^{-1}$  from 1996 to 2009 (Pilegaard et al., 2011), with the net carbon gain hypothesised to be mainly sequestered in woody biomass. At Borden Forest, changes in carbon sequestration may be influenced by changes in forest composition and structure, with LAI increasing from 4.1 to  $4.6 \text{ m}^2 \text{ m}^{-2}$  from 1995 to 2006 (Teklemariam et al., 2009). However, a number of key climate variables also changed steadily and may contribute to the changing carbon dynamics. Air and soil temperature increased by  $0.09 \text{ }^\circ\text{C yr}^{-1}$  and  $0.08 \text{ }^\circ\text{C yr}^{-1}$ , respectively, over the 17 year period. Annual PAR also increased by  $2.5 \mu\text{mol m}^{-2} \text{ s}^{-1} \text{ yr}^{-1}$ . Annual total precipitation remained fairly stable, with a slightly decreasing trend of  $-4.5 \text{ mm yr}^{-1}$ . Warming may impact the forest carbon budget through enhanced respiration and through changes in rates of nutrient cycling, which may lead to long-term increases in  $\text{CO}_2$  uptake (Eliasson et al., 2005; Melillo et al., 2002, 2011).

### 5.2. Carbon uptake period dynamics and annual CO<sub>2</sub> exchange

A number of studies have noted that, with warming climate in northern latitudes, the timing of the plant phenological stages has shifted to earlier in spring and later in autumn, extending the length of the vegetation growing season (Barichivich et al., 2013; Richardson et al., 2010). At Borden Forest, the dynamics of the carbon uptake period varied considerably from year to year, with the start of season varying from DOY 124 to 159, and the end of season from DOY 258 to 292. The overall duration of the carbon uptake period ranged from 111 to 164 days. Relationships of the CUP dates with annual CO<sub>2</sub> budgets were inconclusive (Fig. 4 of Gonsamo et al., 2015; Fig. 8 of this paper). Both GEP and R<sub>E</sub> were negatively correlated with the end of the season; however these correlations were heavily influenced by low GEP and R<sub>E</sub> values in the extremely dry year of 2007 and extremely wet year of 2008. With these years excluded from analysis, there were no significant relationships between R<sub>E</sub> and the start, end, or duration of the CUP, while GEP increased slightly with earlier start of CUP. These inconclusive findings for CUP metrics and annual carbon budgets contrast recent work, which links climate change to changes in plant phenology and thus to ecosystem processes (Churkina et al., 2005; Dragoni et al., 2011; Pan et al., 2011; Richardson et al., 2009, 2010; Wu et al., 2013). The length of the carbon uptake period was found to be the best explanatory phenological metric for annual NEP at Borden Forest ( $R=0.57$ ,  $p<0.01$ ); this correlation is not affected by the inclusion of the two anomalous years that skew the GEP or R<sub>E</sub> relationships with CUP metrics. The complexity of the response of annual net CO<sub>2</sub> fluxes to variability in carbon uptake period may be influenced by site characteristics such as the vegetation species, meteorological variables, water table depth, or soil nitrogen availability. For example, increasing autumn temperatures may prolong the growing season in boreal coniferous forests and other high-latitude ecosystems; however, the autumn warming may have little effect on annual NEP due to light limitations on photosynthesis or respiration losses that exceed any photosynthetic gains (Piao et al., 2008; Richardson et al., 2010; Suni et al., 2003; Wu et al., 2013).

### 5.3. Carbon fluxes in response to environmental controls

The findings from this long-term analysis suggest that the annual CO<sub>2</sub> budgets at Borden Forest are predominantly correlated to PAR ( $R=0.53$ ,  $p<0.01$ ) (Gonsamo et al., 2015). However, during individual seasons other environmental variables are well correlated with NEP, indicating a change throughout the year in the environmental control of ecosystem productivity. Using either monthly or seasonal means, NEP is correlated to VPD and temperature in spring (AM), but to PAR in summer (JJA) and fall (SO) (Fig. 9, and Table 1). The positive relationship between NEP and PAR is likely due to the role of PAR in photosynthetic processes and thus C sequestration, as PAR is absorbed from sunlight by chlorophyll-a and its accessory pigments (chlorophyll-b, carotenoids). In fall, air and soil temperatures were strongly correlated with NEP using monthly means, but not using seasonal means, indicating that temperature influences the cessation of growth toward the end of the season but may have limited influence on interannual variability in carbon uptake.

Respiration showed strong correlations with precipitation and soil temperature in winter and spring (JFM and AM), with reduced R<sub>E</sub> in seasons with cooler temperatures and greater precipitation. The relationship with precipitation may indicate the retarding influence of a heavy snow pack and/or high soil moisture on ecosystem processes. Correlations of respiration with summer environmental variables were generally weaker, indicating the complexity of growing season processes. For example, while there was no statistically significant correlation of R<sub>E</sub> with soil moisture,

Fig. 5 shows large decreases in summer maximum monthly R<sub>E</sub> rates in the middle of the time series, which appear to correspond to several years of summertime low soil moisture content (Fig. 4). Barr et al. (2007) also noted that R<sub>E</sub>, mainly heterotrophic respiration, significantly decreased in drought years at a moderately well drained aspen site in Saskatchewan, Canada. These observations are consistent with a decrease in microbial activity and heterotrophic respiration when volumetric soil water content is low (Ju et al., 2006). Conversely, high soil water content may also limit microbial activity and respiration, as conditions become increasingly anoxic (Ju et al., 2006); while the mean monthly soil moisture never exceeded 0.2 m<sup>3</sup> m<sup>-3</sup> (Fig. 4), high monthly mean values are generally a result of several days or weeks with very high soil moisture values and possible anoxia. These contrasting responses at the two extremes of soil moisture content may explain the poor correlation with respiration at Borden Forest.

Summer GEP was also found to be related to mean soil moisture content ( $R=0.54$ ,  $p<0.05$ ). This was an expected result as soil water content controls transpiration and thus photosynthesis (Harris et al., 2004; Ju et al., 2006). Photosynthesis increases with increasing soil water content, from zero at the wilting point to a peak near field capacity; above the field capacity, photosynthesis decreases slightly (Ju et al., 2006). Consequently, non-drought years are likely to sustain photosynthetic rates longer into the late growing season, assuming other conditions – such as adequate temperatures and light availability – are met. GEP was most strongly correlated with spring environmental variables, including mean spring VPD ( $R=0.74$ ,  $p<0.01$ ) (likely due to correlation of VPD with air temperature) and spring soil temperature ( $R=0.74$ ,  $p<0.01$ ), which may be a proxy for snow melt. The strong springtime relationship of GEP to soil temperature also likely reflects a triggering of C sequestration by long-term, consistent temperature increases, rather than short-term air temperature fluctuations.

### 5.4. Seasonal hysteresis in NEP response

The influence of climate on the productivity of forest ecosystems is highly complex. Barr et al. (2007) noted direct, immediate responses (e.g., the effect of light and temperature on photosynthesis) and indirect or transient responses and feedbacks (e.g., the effect of temperature on leaf physiology). An interesting finding from Borden Forest is the apparent hysteresis of NEP in response to some environmental variables. Hysteresis in the response of NEP to air temperature has been noted in some forests, although this mechanism is relatively unexplored (Niu et al., 2011). While the results from Borden Forest show no seasonal hysteresis for air or soil temperature controls, there was a strong hysteresis for both PAR and VPD. For a given radiation intensity (PAR), springtime NEP was noticeably lower than fall or summer NEP; furthermore, the rate of change of NEP with PAR was higher in fall than in spring. This slow springtime response was likely because the leaves, particularly in deciduous species, are still accumulating chlorophyll and the photosynthetic apparatus following budburst in the early growing season and are not physiologically optimized for photosynthesis. The absence of a hysteric response to air or soil temperature may indicate that temperatures are the dominant environmental drivers of NEP in this system; once favorable temperature conditions are met and the biotic foundations are in place, secondary controls such as VPD and PAR become influential.

## 6. Conclusions

This study presents the meteorological and carbon flux analysis from Borden Forest for a long-term 17-year dataset (1996–2013). Borden Forest is a low-to-moderate sink, with an average CO<sub>2</sub> budget of 177 gC m<sup>-2</sup> yr<sup>-1</sup>, with standard error of

the mean of  $28 \text{ gC m}^{-2} \text{ yr}^{-1}$  and net sequestration increasing by  $15.7 \text{ gC m}^{-2} \text{ yr}^{-1}$  per year. This provides more evidence contradicting traditional assumptions that mature forests are C neutral and not important as sinks in the global carbon budget (Carey et al., 2001; Luysaert et al., 2008). In two years, however, Borden Forest was a weak carbon source ( $-36 \text{ gC m}^{-2} \text{ yr}^{-1}$  in 1996 and  $-35 \text{ gC m}^{-2} \text{ yr}^{-1}$  in 2001), indicating that the ecosystem can switch quickly from a carbon sink to a carbon source in response to environmental or climatic drivers. A long-term warming trend was observed in both air temperature ( $0.09^\circ\text{C yr}^{-1}$ ,  $R=0.52$ ,  $p<0.05$ ) and soil temperature ( $0.08^\circ\text{C yr}^{-1}$ ,  $R=0.71$ ,  $p<0.001$ ). Photosynthetically active radiation and soil temperature were found to have the strongest correlation with interannual variability in NEP, particularly in the June–August season ( $R=0.61$ ,  $p<0.01$  and  $R=0.45$ ,  $p<0.05$ , respectively). Annual NEP values were related to length of the growing season ( $R=0.57$ ,  $p<0.01$ ), with a longer carbon uptake period (CUP) leading to more biomass accumulation. However, the relationship of NEP and its component fluxes with start, end, or duration of the growing season is not straightforward, due to variability in environmental conditions within the growing season. We have focused here on identifying trends and possible drivers of carbon exchange, but note both the interdependencies among environmental variables and the temporal complexity of the ecosystem response; further investigation beyond the scope of this paper,

using multivariate model-data fusion, may yield additional insights into the underlying mechanisms controlling annual and seasonal carbon budgets. The meteorological and carbon flux results from this long-term dataset demonstrate the importance of monitoring the feedbacks among climate, ecosystems, and carbon flux; this information may help to predict future shifts under anthropogenic climate change.

### Acknowledgements

The authors gratefully acknowledge the technical field support by Patrick Lee, Paul Bartlett, Andrew Elford, John Deary and Jim Arnold, and CFB Borden for hosting the flux site. Funding for the research was provided primarily by Environment Canada. NF acknowledges computer resources and research time provided by Northern Michigan University, HC and JC thank the National Sciences and Engineering Research Council of Canada for partial support through a Discovery Grant, and AG thanks NSFC Research Fund for International Young Scientists (grant no. 41450110076).

### Appendix A.

#### Instrumentation at Borden.

Category	Measurement	Manufacturer	Instrument	Height(s)	Dates
Fluxes	3-D wind, sonic temperature	Kaijo Denki Campbell Sci. Applied Technologies Inc.	DAT-310	33.4 m	06/95–04/01
			CSAT	33.4 m	04/01–12/03
	CO <sub>2</sub> and H <sub>2</sub> O	LI-COR Inc.	Type K	33.4 m	04/05–present
			LI-6262	Inlet at 33.4 m	07/05–12/03; 04/05–present
Radiation	Net radiation 4-component net radiation Incoming Shortwave Incoming PAR	Middleton Instr. Kipp & Zonen Inc.	CN1-R	44 m	06/95–12/03
			CNR-1	33.7 m	06/00–12/03
		Eppley Lab	PSP	44 m	04/05–present
			LI-COR Inc.	LI-190SA	44 m
	Reflected PAR	LI-COR Inc.	LI-191 line quantum sensor	41.5 m	04/05–present
			LI-190SA	41.5 m	04/05–present
		LI-COR Inc.	LI-191 line quantum sensor	1.5 m	07/98–12/03; 04/05–present
			LI-190SA	33.6 m	04/05–present
Meteorology	Wind speed & direction	RM Young Co.	Model 05103	44 m	06/95–12/03
				43 m	04/05–present
	Temperature & relative humidity	Rotronic Instr. Corp. Vaisala Vaisala	MP-100	41, 33 m	06/95–12/03
			HMP-35C	41, 33 m	04/05–08/05
			HMP-45C	41, 33 m	08/05–present
	Temperature profile	Setra	Ventilated thermocouples	41, 33, 29, 26, 23, 20, 16, 13, 10, 6, 3, 1.5 m	06/95–12/03; 04/05–present
			270	2 m	06/95–12/03; 04/05–present
Gas profile	CO <sub>2</sub> and H <sub>2</sub> O	LI-COR Inc.	Li-6262	34, 25, 18, 10, 5, 1 m	01/01–12/03;
				33, 26, 18, 10, 5, 1 m	04/05–04/08
				42, 33, 26, 17, 5, 1 m	04/08–present
	O <sub>3</sub> SO <sub>2</sub>	Thermal Environmental Inc. Thermal Environmental Inc.	Model 49 Model 43	Same as CO <sub>2</sub> Same as CO <sub>2</sub>	Same as CO <sub>2</sub> 04/05–present
Soil & Boles	Soil temperature	Campbell Sci.	107 thermistors	Site 1: 5, 10, 20, 50, 100 cm;	07/05–12/03;
			Thermocouples	Site 2: 5 cm	04/05–present
	Soil heat flux	Campbell Sci.	HFP01	Site 2: 10, 20, 50, 100 cm	07/05–12/03;
				7.5 cm (3 sites)	04/05–present
	Soil moisture	Campbell Sci.	CS615	2, 5, 10, 20, 50, 100 cm (2 sites)	07/97–11/03;
				2, 5, 10 m (red maple); 2, 5, 9 m (aspen)	04/05–present
Bole temperatures	Campbell Sci.	107 thermistors	2, 5, 10 m (red maple); 2, 5, 9 m (aspen)	08/95–12/03; 04/05–present	

## References

- Allard, V., Ourcival, J.M., Rambal, S., Joffre, R., Rocheteau, A., 2008. Seasonal and annual variation of carbon exchange in an evergreen Mediterranean forest in southern France. *Global Change Biol.* 14 (4), 714–725.
- Baldocchi, D., 2008. Turner review no. 15. Breathing of the terrestrial biosphere: lessons learned from a global network of carbon dioxide flux measurement systems. *Aust. J. Bot.* 56, 1–26.
- Barichivich, J., Briffa, K.R., Myneni, R.B., Osborn, T.J., Melvin, T.M., Ciais, P., et al., 2013. Large-scale variations in the vegetation growing season and annual cycle of atmospheric CO<sub>2</sub> at high northern latitudes from 1950 to 2011. *Global Change Biol.* 19 (10), 3167–3183.
- Barr, A.G., Black, T.A., Hogg, E.H., Griffiths, T.J., Morgenstern, K., Kljun, N., et al., 2007. Climatic controls on the carbon and water balances of a boreal aspen forest, 1994–2003. *Global Change Biol.* 13 (3), 561–576.
- Barr, A.G., Black, T.A., Hogg, E.H., Kljun, N., Morgenstern, K., Nesic, Z., 2004. Inter-annual variability in the leaf area index of a boreal aspen-hazelnut forest in relation to net ecosystem production. *Agric. For. Meteorol.* 126, 237–255.
- Barr, A.G., Richardson, A.D., Hollinger, D.Y., Papale, D., Arain, M.A., Black, T.A., et al., 2013. Use of change-point detection for friction-velocity threshold evaluation in eddy-covariance studies. *Agric. For. Meteorol.* 171–172, 31–45.
- Beer, C., Reichstein, M., Tomelleri, E., Ciais, P., Jung, M., Carvalhais, N., et al., 2010. Terrestrial gross carbon dioxide uptake: global distribution and covariation with climate. *Science* 329 (5993), 834–838.
- Black, T.A., Chen, W.J., Barr, A.G., Arain, M.A., Chen, Z., Nesic, Z., et al., 2000. Increased carbon sequestration by a boreal deciduous forest in years with a warm spring. *Geophys. Res. Lett.* 27 (9), 1271–1274.
- Blanken, P.D., Black, T.A., Yang, P.C., Neumann, H.H., Nesic, Z., Staebler, R., et al., 1997. Energy balance and canopy conductance of a boreal aspen forest: partitioning overstory and understory components. *J. Geophys. Res.* 102 (D24), 28915–28927.
- Carey, E.V., Sala, A., Keane, R., Callaway, R.M., 2001. Are old forests underestimated as global carbon sinks? *Global Change Biol.* 7 (4), 339–344.
- Churkina, G., Schimel, D., Braswell, B.H., Xiao, X., 2005. Spatial analysis of growing season length control over net ecosystem exchange. *Global Change Biol.* 11 (10), 1777–1787.
- Coursolle, C., Margolis, H.A., Giasson, M.-A., Bernier, P.-Y., Amiro, B.D., Arain, M.A., et al., 2012. Influence of stand age on the magnitude and seasonality of carbon fluxes in Canadian forests. *Agric. For. Meteorol.* 165, 136–148.
- Croft, H., Chen, J.M., Zhang, Y., 2014. Temporal disparity in leaf chlorophyll content and leaf area index across a growing season in a temperate deciduous forest. *Int. J. Appl. Earth Obs. Geoinf.* 33, 312–320.
- Dragoni, D., Schmid, H.P., Wayson, C.A., Potter, H., Grimmond, C.S.B., Randolph, J.C., 2011. Evidence of increased net ecosystem productivity associated with a longer vegetated season in a deciduous forest in south-central Indiana, USA. *Global Change Biol.* 17 (2), 886–897.
- Eliasson, P.E., McMurtrie, R.E., Pepper, D.A., Strömberg, M., Linder, S., Ågren, G.I., 2005. The response of heterotrophic CO<sub>2</sub> flux to soil warming. *Global Change Biol.* 11 (1), 167–181.
- Fischelli, N.A., Froelich, L.E., Reich, P.B., 2013. Climate and interrelated tree regeneration drivers in mixed temperate-boreal forests. *Landscape Ecol.* 28 (1), 149–159.
- Froelich, L.E., Reich, P.B., 2010. Will environmental changes reinforce the impact of global warming on the prairie-forest border of central North America? *Front. Ecol. Environ.* 8 (7), 371–378.
- Goldblum, D., Rigg, L., 2005. Tree growth response to climate change at the deciduous-boreal forest ecotone, Ontario, Canada. *Can. J. For. Res.* 35 (11), 2709–2718.
- Goldblum, D., Rigg, L., 2010. The deciduous forest – boreal forest ecotone. *Geogr. Compass* 4, 701–717.
- Gonsamo, A., Chen, J.M., Wu, C., Dragoni, D., 2012. Predicting deciduous forest carbon uptake phenology by upscaling fluxnet measurements using remote sensing data. *Agric. For. Meteorol.* 165, 127–135.
- Gonsamo, A., Croft, H., Chen, J.M., Wu, C., Froelich, N., Staebler, R.M., 2015. Radiation contributed more than temperature to increased decadal autumn and annual carbon uptake of two eastern North America mature forests. *Agric. For. Meteorol.* 201, 8–16.
- Goulden, M.L., Munger, J.W., Fan, S.-M., Daube, B.C., Wofsy, S.C., 1996. Exchange of carbon dioxide by a deciduous forest: response to interannual climate variability. *Science* 271 (5255), 1576–1578.
- Granier, A., Reichstein, M., Bréda, N., Janssens, I.A., Falge, E., Ciais, P., et al., 2007. Evidence for soil water control on carbon and water dynamics in European forests during the extremely dry year: 2003. *Agric. For. Meteorol.* 143 (1–2), 123–145.
- Greco, S., Baldocchi, D.D., 1996. Seasonal variations of CO<sub>2</sub> and water vapour exchange rates over a temperate deciduous forest. *Global Change Biol.* 2 (3), 183–197.
- Harris, P.P., Huntingford, C., Cox, P.M., Gash, J.H., Malhi, Y., 2004. Effect of soil moisture on canopy conductance of Amazonian rainforest. *Agric. For. Meteorol.* 122 (3–4), 215–227.
- Hollinger, D.Y., Aber, J., Dail, B., Davidson, E.A., Goltz, S.M., Hughes, H., et al., 2004. Spatial and temporal variability in forest-atmosphere CO<sub>2</sub> exchange. *Global Change Biol.* 10 (10), 1689–1706.
- Ju, W., Chen, J.M., Black, T.A., Barr, A.G., Liu, J., Chen, B., 2006. Modelling multi-year coupled carbon and water fluxes in a boreal aspen forest. *Agric. For. Meteorol.* 140 (1–4), 136–151.
- Lee, X.H., Fuentes, J.D., Staebler, R.M., Neumann, H.H., 1999. Long-term observation of the atmospheric exchange of CO<sub>2</sub> with a temperate deciduous forest in southern Ontario, Canada. *J. Geophys. Res.* 104 (D13), 15975–15984.
- Leithhead, M.D., Anand, M., Silva, L.C.R., 2010. Northward migrating trees establish in treefall gaps at the northern limit of the temperate-boreal ecotone, Ontario, Canada. *Oecologia* 164 (4), 1095–1106.
- Luyssaert, S., Schulze, E.-D., Börner, A., Knohl, A., Hessenmöller, D., Law, B.E., et al., 2008. Old-growth forests as global carbon sinks. *Nature* 455 (7210), 213–215.
- Melillo, J.M., Butler, S., Johnson, J., Mohan, J., Steudler, P., Lux, H., et al., 2011. Soil warming, carbon-nitrogen interactions, and forest carbon budgets. *Proc. Natl. Acad. Sci. U. S. A.* 108 (23), 9508–9512.
- Melillo, J.M., Steudler, P.A., Aber, J.D., Newkirk, K., Lux, H., Bowles, F.P., et al., 2002. Soil warming and carbon-cycle feedbacks to the climate system. *Science* 298 (5601), 2173–2176.
- Neumann, H.H., Den Hartog, G., Shaw, R.H., 1989. Leaf area measurements based on hemispheric photographs and leaf-litter collection in a deciduous forest during autumn leaf-fall. *Agric. For. Meteorol.* 45 (3–4), 325–345.
- Niu, S., Luo, Y., Fei, S., Montagnani, L., Bohrer, B., Janssens, I.A., et al., 2011. Seasonal hysteresis of net ecosystem exchange in response to temperature change: patterns and causes. *Global Change Biol.* 17 (10), 3102–3114.
- Nobrega, S., Grogan, P., 2007. Deeper snow enhances winter respiration from both plant-associated and bulk soil carbon pools in birch hummock tundra. *Ecosystems* 10 (3), 419–431.
- Oliphant, A.J., Grimmond, C.S.B., Zutter, H.N., Schmid, H.P., Su, H.-B., Scott, S.L., et al., 2004. Heat storage and energy balance fluxes for a temperate deciduous forest. *Agric. For. Meteorol.* 126 (3–4), 185–201.
- Pan, Y., Birdsey, R.A., Fang, J., Houghton, R., Kauppi, P.E., Kurz, W.A., et al., 2011. A large and persistent carbon sink in the world's forests. *Science* 333 (6045), 988–993.
- Piao, S., Ciais, P., Friedlingstein, P., Peylin, P., Reichstein, M., Luyssaert, S., et al., 2008. Net carbon dioxide losses of northern ecosystems in response to autumn warming. *Nature* 451 (7174), 49–52.
- Pilegaard, K., Ibrom, A., Courtney, M.S., Hummelshøj, P., Jensen, N.O., 2011. Increasing net CO<sub>2</sub> uptake by a Danish beech forest during the period from 1996 to 2009. *Agric. For. Meteorol.* 151 (7), 934–946.
- Richardson, A.D., Andy Black, T., Ciais, P., Delbart, N., Friedl, M.A., Gobron, N., et al., 2010. Influence of spring and autumn phenological transitions on forest ecosystem productivity. *Philos. Trans. R. Soc. B: Biol. Sci.* 365 (1555), 3227–3246.
- Richardson, A.D., Hollinger, D.Y., Dail, D.B., Lee, J.T., Munger, J.W., O'keefe, J., 2009. Influence of spring phenology on seasonal and annual carbon balance in two contrasting new England forests. *Tree Physiol.* 29 (3), 321–331.
- Saigusa, N., Yamamoto, S., Murayama, S., Kondo, H., Nishimura, N., 2002. Gross primary production and net ecosystem exchange of a cool-temperate deciduous forest estimated by the eddy covariance method. *Agric. For. Meteorol.* 112 (3–4), 203–215.
- Schotanus, P., Nieuwstadt, F., de Bruin, H., 1983. Temperature measurement with a sonic anemometer and its application to heat and moisture fluxes. *Boundary-Layer Meteorol.* 26, 81–93.
- Staebler, R.M., Fitzjarrald, D.R., 2004. Observing subcanopy CO<sub>2</sub> advection. *Agric. For. Meteorol.* 122 (3–4), 139–156.
- Staebler, R.M., Fuentes, J.D., Lee, X.H., Puckett, K.J., Neumann, H.H., Deary, J.A., 2000. Long term flux measurements at the Borden forest. *CMOS Bull.* 28 (1), 9–16.
- Suni, T., Berninger, F., Markkanen, T., Keronen, P., Rannik, Ü., Vesala, T., 2003. Interannual variability and timing of growing-season CO<sub>2</sub> exchange in a boreal forest. *J. Geophys. Res.: Atmos.* 108 (D9), 4265.
- Teklemariam, T., Staebler, R.M., Barr, A.G., 2009. Eight year of carbon dioxide exchange above a mixed forest at Borden, Ontario. *Agric. For. Meteorol.* 149 (11), 2040–2053.
- Urbanski, S., Barford, C., Wofsy, S., Kucharik, C., Pyle, E., Budney, J., et al., 2007. Factors controlling CO<sub>2</sub> exchange on timescales from hourly to decadal at Harvard forest. *J. Geophys. Res.: Biogeosci.* 112 (G2), G02020.
- Wang, X., Piao, S., Ciais, P., Li, J., Friedlingstein, P., Koven, C., et al., 2011. Spring temperature change and its implication in the change of vegetation growth in North America from 1982 to 2006. *Proc. Natl. Acad. Sci. U. S. A.* 108 (4), 1240–1245.
- Webb, E.K., Pearman, G.I., Leuning, R., 1980. Correction of flux measurements for density effects due to heat and water vapour transfer. *Q. J. R. Meteorol. Soc.* 106 (447), 85–100.
- Wu, C., Chen, J.M., Black, T.A., Price, D.T., Kurz, W.A., Desai, A.R., et al., 2013. Interannual variability of net ecosystem productivity in forests is explained by carbon flux phenology in autumn. *Global Ecol. Biogeogr.* 22 (8), 994–1006.
- Wu, C., Gonsamo, A., Chen, J.M., Kurz, W.A., Price, D.T., Lafleur, P.M., et al., 2012. Interannual and spatial impacts of phenological transitions, growing season length, and spring and autumn temperatures on carbon sequestration: a North America flux data synthesis. *Global Planet. Change* 92–93, 179–190.
- Yi, C., Ricciuto, D., Li, R., Wolbeck, J., Xu, X., Nilsson, M., et al., 2010. Climate control of terrestrial carbon exchange across biomes and continents. *Environ. Res. Lett.* 5 (3), 34007.
- Zha, T.S., Barr, A.G., Bernier, P.-Y., Lavigne, M.B., Trofymow, J.A., Amiro, B.D., et al., 2013. Gross and aboveground net primary production at Canadian forest carbon flux sites. *Agric. For. Meteorol.* 174–175, 54–64.